Available online at www.sciencedirect.com
ScienceDirect
Thermochimica Acta 470 (2008) 27–35
thermochimica acta
www.elsevier.com/locate/tca

Thermal and topographical characterization of polyester- and styrene/acrylate-based composite powders by scanning probe microscopy

Kaj Backfolk [a,*], Petri Sirviö [a,b], Petri Ihalainen [b], Jouko Peltonen [c]

[a] *Stora Enso Oyj, Imatra Research Centre, FI-55 800 Imatra, Finland*
[b] *Department of Physical Chemistry, Åbo Akademi University, Porthaninkatu 3-5, FI-20500 Turku, Finland*
[c] *Laboratory of Paper Coating and Converting, Åbo Akademi University, Porthaninkatu 3-5, FI-20500 Turku, Finland*

Received 4 July 2007; received in revised form 30 November 2007; accepted 13 January 2008
Available online 1 February 2008

Abstract

The thermal properties of two conventional polyester-based toners and a chemically prepared styrene/acrylate toner with different thermal histories were studied by scanning probe microscopy (SPM) and differential scanning calorimetry (DSC). The thermal transition temperatures detected by SPM agreed with the results of the DSC measurements. The validity of SPM for detecting thermal transitions was further confirmed by studying two amorphous reference polymers with different glass transition points (T_g) and three crystalline reference polymers with different melting points (T_m). When the toner sample was heated by the SPM probe above the glass transition temperature of the toner powder ($T_{probe} > T_g$), changes occurred in the surface topography and roughness causing different levels of local sintering of the particles. A set of roughness parameters calculated from the SPM image data were used to quantify the most essential features of toner surfaces. Environmental scanning electron microscopy (ESEM) was used to study the penetration depth of heat dissipated by the SPM probe. The probe-annealing was compared with oven-annealing in order to establish the effect of thermal history on the thermal properties of the materials.

Keywords: Thermal analysis; Toner; Binder; Glass transition temperature; Topography; DSC; ESEM; SPM

1. Introduction

Toner melting, sintering, spreading or leveling and penetration are the main physical stages associated with the fusing process in dry toner electrophotography [1,2]. The progress of these stages has been illustrated with oven-fused samples showing that melting and sintering of the toner particles occurs before fixing to the substrate [3]. The initial phases of the fusing process, i.e. melting and sintering are mainly dictated by the toner properties and fusing conditions. The subsequent spreading, leveling and penetration stage is a complex interplay between fusing conditions, toner properties and the physical and physico-chemical properties of the substrate. The spreading and leveling of toners on different substrates and the effect on print quality have been shown to be dependent not only on the fusing conditions but also on the surface energy of the substrate [4–7]. The substrate or surface compressibility may also affect the contact area, dwell time and fusing nip temperature [8]. Different opinions have been presented concerning the effect of surface roughness on the fusing fix [9,10]. The toner penetration depth is in the range of micrometers in roll fusing systems on uncoated paper [6,11], and this is obviously strongly influenced by the thermo-rheological properties of the toners.

The relationship between the rheological properties of toners and the fusing fix [12,13] suggests that toner leveling and maximum substrate contact are essential for toner adhesion. Since the surface roughness affects both toner packing and heat absorption ability, surface (toner/air) and interface (toner/substrate) temperatures should be optimal in order to achieve proper conditions for particle sintering and coalescence [14]. In addition, changes in fusing nip temperature in the printing direction due to local differences in thermal diffusivity [15], and cross-section temperature gradients caused by particle size effects [16] make it difficult to achieve optimal fusing conditions.

* Corresponding author. Tel.: +358 2046 23467.
E-mail address: Kaj.Backfolk@storaenso.com (K. Backfolk).

0040-6031/$ – see front matter © 2008 Elsevier B.V. All rights reserved.
doi:10.1016/j.tca.2008.01.013

Nevertheless, only a limited number of methods have been developed to gain information about toner properties at elevated temperatures related to their sintering, leveling and spreading behavior. Rheological characterization is often used to describe toner properties important for runnability and print quality. Differential scanning calorimetry (DSC) and dynamic mechanical analysis (DMA) have been used for the thermal analysis of toners. The spreading of individual toner particles on different glass substrates has been studied in a microscope [4] and Lever and Price [17] have utilized micro-thermomechanical analysis (μTMA) and micro-modulated differential thermal analysis (μMDTA) to study the thermal properties of toner particles. In addition, thermal properties and glass transition temperatures of polymer and composite films have been studied by utilizing various modes of SPM, such as scanning thermal microscopy (SThM) [18–24], local thermal analysis (LTA) [25,26], friction (later) force microscopy [27–29], shear-modulated scanning force microscopy (SM-SFM) [30,31], scanning local acceleration microscopy (SLAM) [32], and various spectroscopic modes including force–distance measurements [33] and an SPM probe resonance frequency method by utilizing an SPM probe as a sensor for detecting thermal transitions [34–37].

A novel method for the thermal characterization of latex films utilizing scanning probe microscopy (SPM) was recently presented [38–40]. In this non-contact approach, the SPM probe is heated and the probe is utilized simultaneously as an actuator and a sensor. The heated probe both dissipates heat and detects the heat reflected from the sample. The resonance frequency (ω) of the probe oscillating above the sample surface is determined for different probe temperatures (T_p). The $\Delta\omega$–T_p curves can be used to detect thermal transitions in latex films as changes in the heat capacity of the samples [38]. The direction of the temperature gradient can be chosen, i.e. towards the sample (probe heating) or from the sample (sample heating), so that migration or evaporation from the bulk can be identified and taken into account.

In the present study, the SPM probe frequency method [38] has been used to determine thermal properties of dry toner powder samples. Two conventional toners consisting of a polyester binder and a chemically prepared toner containing styrene-butyl acrylate binder were studied. The SPM probe frequency method was validated by comparing thermal transition temperatures obtained by SPM with those obtained by DSC. In addition to the three toner samples, three crystalline polymers and two amorphous polymers were used as references. The various toner powder samples were also oven-annealed before SPM thermal analysis in order to establish the effect of sintering, i.e. thermal history, on the thermal properties of the materials. In addition to thermal analysis, FTIR spectroscopy, and topography and phase contrast imaging of toner tablet surfaces were studied. A set of roughness parameters calculated from the SPM image data were used to quantify the most essential features of toner surfaces. Environmental scanning electron microscopy (ESEM) was used to study the penetration depth of heat dissipated by the SPM probe.

2. Experimental

2.1. Materials

Three types of commercial toners were collected directly as powders from the cartridges of different electrophotographic machines. Toner 1 was a conventional black toner with a polyester type binder, toner 2 was a conventional cyan toner with a polyester type of binder similar to that of sample 1, and toner 3 was a chemically prepared toner containing a styrene/butyl acrylate binder. The toner powders were pressed to a tablet before determining the thermal properties with SPM. In order to study the effect of thermal history, the pressed toner tablets were heat-treated or sintered as a film on mica in an oven at 160 °C for 10 min (referred to as oven-annealing).

Three crystalline reference polymers used for the thermal study were; a copolymer of ethylene and methacrylic acid (15 wt%) (Nucrel® 925, Dupont™), a copolymer of ethylene and methacrylic acid (11 wt%) (Nucrel® 699, Dupont™), and a ethylene-vinyl acetate (28 wt%)/acid terpolymer resin (Elvax® 4260, DuPont™), denoted reference 1, 2, 3, respectively. Two amorphous styrene/butadiene latex polymers with low and high-glass transition temperatures were used. The first copolymer, denoted reference 4, consisted of a mixture of styrene (82.6 wt%) and butadiene (15.0 wt%) and the second copolymer, denoted reference 5, consisted of a mixture of styrene and butadiene with a ratio of 92.8:5.0 wt% [38]. Both were supplied by Omnova Solution Inc. (USA).

2.2. Methods

A Nanoscope IIIa (Digital Instruments Veeco Metrology Group, Santa Barbara, CA) SPM equipped with a MultiMode™ high temperature heater was used for imaging and thermal analysis of the sample surfaces. Both the sample and the cantilever (probe) can be heated, either simultaneously or separately, from ambient temperature up to 250 °C [41–43]. A specialized AS-130VT scanner including a resistive type heater and a thermocouple for sample temperature measurement was used. The scanner contains a water–fluid cooling system to protect the piezo elements from overheating. Uncoated 0.01–0.025 Ω cm antimony (*n*)-doped silicon probes (model LTESP, Veeco) were used for thermal analysis and imaging. The probes were installed in a special probe holder with options for cantilever oscillation and probe heating, gas purging and external sensor access. The microscope was placed on an active vibration isolation table (MOD-1M JRS Scientific Instruments, Switzerland) mounted on a massive stone table to eliminate external vibrational noise.

All the images (512 × 512 pixels) were captured using intermittent contact under ambient conditions (25 ± 3 °C, 35 ± 5% RH) without filtering. The free amplitude of the oscillating cantilever (off contact) was set to 70 ± 5 nm. The engage procedure caused a shift in the resonance frequency, which was taken into account. The new resonance frequency for the tip in contact was determined and used as the operating frequency. A damping ratio (measuring amplitude/free amplitude) of 0.5–0.6 was used for imaging. The scanning probe image processor

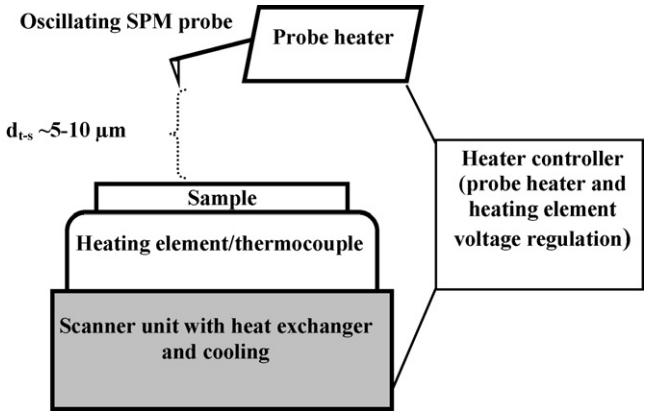

Scheme 1. A schematic illustrating the set-up used for the SPM probe heating and sample heating (not in scale). The schema also shows the approximated distance between the tip and the sample (d_{t-s}) during measurement.

(SPIP, Image Metrology, Denmark) software was used for the roughness analysis. Roughness parameters were calculated from 25 μm × 25 μm topographic images. Before the roughness analysis, LMS polynomial plane fitting (1st order) was applied to the unprocessed images.

The heating-by-the-sample and heating-by-the-probe methods have been described previously in detail [38]. In this work, the heating-by-the-probe method was used. The sample was mounted on the heating element, but the element was not heated (Scheme 1). The temperature of the probe was adjusted by applying a voltage to the probe heater with the Nanoscope™ heater controller. The voltage was increased at a constant rate of 0.2 V per 5 min (~0.2 °C/min). The non-contact measurement was made with a tip-sample distance of about 5 μm. In probe-heating mode the probe is heated by applying a voltage (U) to probe heater with the heater controller. The temperature of the probe (T_p) is determined by an empirically obtained approximated polynomial function: $T_p \approx 0.375U^2 + 1.664U - 0.162 + T_0$, where T_0 is the ambient (room) temperature measured simultaneously with the frequency of the probe at each measuring point [41–43]. On the other hand, in the sample-heating mode (not used here) the sample is heated by applying a voltage (U) to the heating element. The temperature of the sample (T_s) can be approximated to be equal to temperature of the heating element (measured by a thermocouple) when the sample is relative thin and small [41].

Table 1
The slope and T_c-values from $\Delta\omega$–T_p curves for toners

Sample number	Slope 1 (Hz/°C)	Slope2 (Hz/°C)	T_c (°C)
Toner 1 (powder tablet)	−10.1 ± 1.5	−6.2 ± 0.2	65.0
Toner 1 (oven-annealed)	−8.1 ± 0.3	−6.1 ± 0.3	65.7
Toner 2 (powder tablet)	−13.6 ± 0.3	−3.5 ± 0.2	74.2
Toner 2 (oven-annealed)	−7.1 ± 0.1	−6.2 ± 0.1	71.8
Toner 3 (powder tablet)	−7.6 ± 0.1	−5.5 ± 0.1	73.4
Toner 3 (oven-annealed)	−6.9 ± 0.1	−5.8 ± 0.1	63.7

Slopes 1 and 2 refer to the slopes below and above the transition temperature

Differential scanning calorimetry (DSC) (Mettler Toledo Stare System DSC 821e Module) was used to determine the glass transition of the toner samples. The temperature scan rate was 10 °C per minute with the following scan sequence: 20–200–20–200 °C. Glass transitions or melting points were determined from the second run. Environmental scanning electron microscope (FEI quanta 200) was used to capture images of the toner samples before and after thermal analysis with the SPM. The images were captured in high vacuum using an ETD detector with an accelerating voltage of 10.0 kV, and 400× and 3000× magnifications. FTIR spectroscopy was used to record chemical fingerprints of the samples before and after the thermal treatment.

3. Results and discussion

3.1. Thermal analysis of toner particles

The toner samples were studied with the heating-by-the-probe method [38] before and after oven-annealing. Typical $\Delta\omega$–T_p-curves are shown in Figs. 1–3 and values obtained from the curves are compiled in Table 1. The critical transition temperatures (T_c) were determined as intersection points of the extrapolated lines obtained by a linear fit to the data points. Slope 1 and slope 2 refer to the slopes below and above the transition temperature. The relatively small standard deviation (<5%) of the average slope values (three samplings) and the T_c

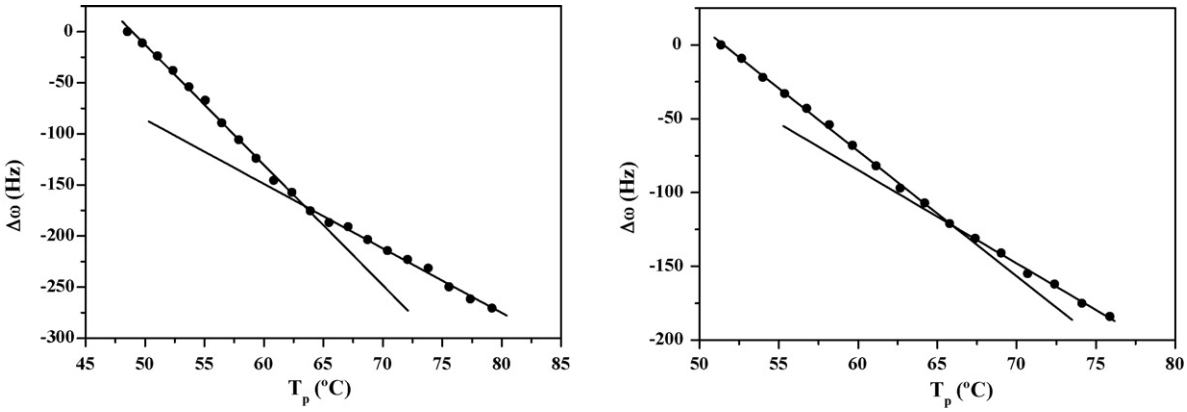

Fig. 1. Typical $\Delta\omega$–T_p curves for toner 1 tablet before (left) and after (right) oven-annealing. The solid lines represent a linear fit to the data points.

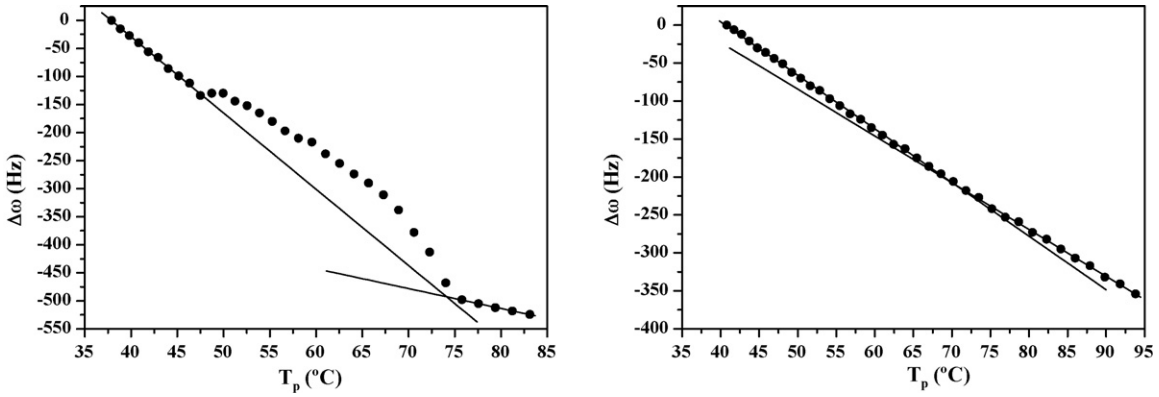

Fig. 2. Typical $\Delta\omega$–T_p curves for toner 2 tablet before (left) and after (right) oven-annealing. The solid lines represent a linear fit to the data points.

values (Table 1) demonstrates the good reproducibility of the measurements.

The change in the slope of the $\Delta\omega$–T_p-curve at T_c has been previously interpreted to correspond to a change in heat capacity of the system [38]. The values of slope 1 of the conventional toner powder (tablet) samples (toners 1 and 2) measured before oven-annealing were clearly more negative than that of toner 3 (Table 1), indicating that the toner samples containing a polyester binder (toners 1 and 2) were less heat absorbing than the toner with a styrene/butyl acrylate binder (toner 3). The slope values of all the toner samples decreased as a result of oven-annealing and the differences between the toners became much smaller (Table 1). This indicates that the effective heat capacity of the composite matrices were quite similar after oven-annealing.

Only one transition was observed for each sample within the measured temperature range (Figs. 1–3). The T_c values for the oven-annealed and non-annealed samples were found to be the same only for toner 1. The T_c of toner 3 had decreased by almost 10 °C as a result of oven-annealing (Table 1). The sensitivity of the system for annealing was hence clearly characteristic of the toner type. Possible reasons for the downward shift of the T_c point might be the change in particle packing and a thermomechanical degradation of styrene–acrylate copolymer [44] alternatively phase segregation of low volatile components during annealing.

Evaporation of water from the sample has been shown to contribute to the slope values and to the magnitude of the transition [38]. Presence of moisture content can thus cause in high evaporative cooling of the probe appearing as a distinct deviation from linearity in the $\Delta\omega$–T_p curve. Such phenomenon was observed for toner 2 within a wide temperature range from 47.5 to 75.8 °C, which might indicate water evaporation causing an increase of T_c, when comparing the value of 74.2 °C with that of the corresponding oven-annealed sample (71.8 °C). The result suggests that a glass transition involving a change of heat capacity may occur only when a major fraction of water has evaporated from the sample. Marked water evaporation has been reported to involve structural rearrangements, an increase of glass-transition temperature and a change of heat capacity [45], in agreement with our findings.

The values of slope 2 were smaller than slope 1 values and were very similar for all the samples whether or not they had been oven-annealed. The effective heat capacity of the toner samples after SPM probe annealing were thus almost the same. The only exception was the non-annealed toner 2 sample, which exhibited clearly the lowest slope 2 value and also the highest slope 1 value (Table 1). In fact, the slope 2 value was lower than the estimated background (limiting slope value) value of ∼−5.0 Hz/°C due to the probe heating by the external voltage [43]. This indicates that the probe was cooled by the extensive evaporation of water from the sample during SPM probe annealing.

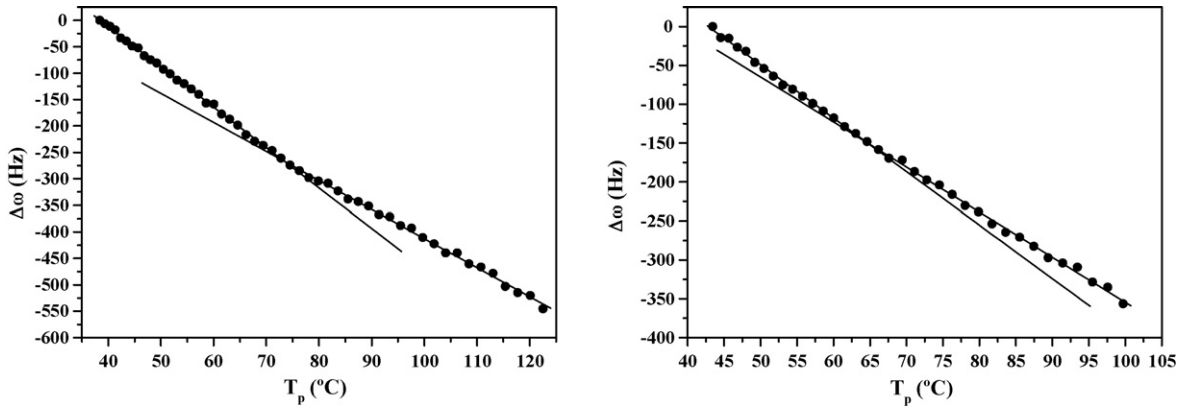

Fig. 3. Typical $\Delta\omega$–T_p curves for toner 3 tablet before (left) and after (right) oven-annealing. The solid lines represent a linear fit to the data points.

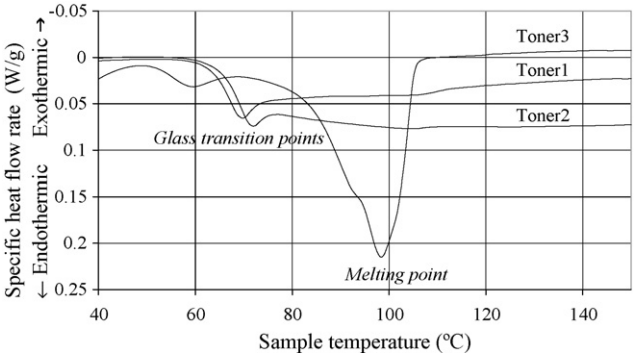

Fig. 4. Glass transition temperatures measured for the studied toners with DSC at a scan rate of 10 °C/min. The curves in the figure correspond to the second heating cycle.

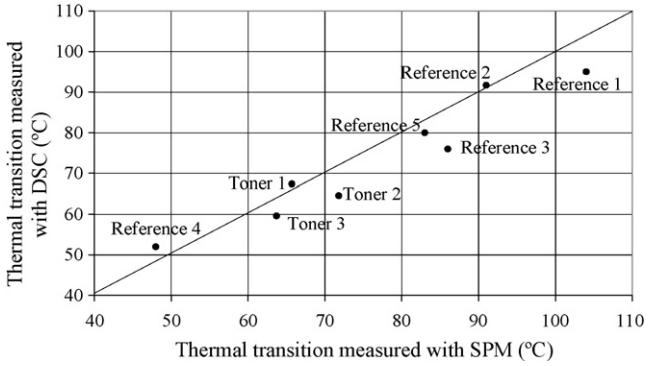

Fig. 5. The thermal transitions (glass transition temperatures and melting points) observed for toners and model polymers by DSC and SPM.

The results indicate that all the studied toner samples reach their maximum thermal absorptivity (within the studied temperature range) above T_c. Furthermore, the oven-annealed samples had not reached the maximum thermal absorptivity as evidenced by the transition still present during probe-annealing. Considering this, the slow heating (0.2 °C/min) at low temperatures (below T_c) with an SPM probe appeared to be more effective than short-time oven-annealing (10 min) at high temperature (clearly above T_c) in reaching the maximum thermal absorptivity.

The thermal history of a sample could be concluded from the transition temperature and the change in heat capacity. The value of slope 1 decreased in the order toner 2, toner 1, toner 3. Since the particle size and size distribution [16] as well as additives such as waxes change the thermal response, in particular in the initial phase of the sintering process, it is important to follow the thermal behavior throughout the process until the immobile sintered phase has been reached. The ability of the samples to absorb heat is expected to increase as a result of sintering of the particles and also as a result of increasing temperature which increases the thermal conductivity [46].

Fig. 4 shows the DSC curves for the samples obtained with a scan rate of 10 °C/min. It has been shown that the T_c detected by the heating-by-the-probe method is not influence by possible volume relaxation occurring at the vicinity of T_g [38]. The shown thermograms are those obtained after the second heating run in order to minimize the magnitude of the kinetic component and enable the detection of changes occurring in the thermodynamic component. This makes the T_g values obtained with DSC automatically more comparable to the T_c values obtained for oven-annealed samples. Furthermore, Toners 1 and 2 exhibit a T_g at approximately 67 and 65 °C, while toner 3 exhibits a glass transition at 60 °C and a strong endothermic peak corresponding to a melting point close to 100 °C. The melting point peak is related to the polyethylene type of wax which was not present in the polyester-based toners. FTIR bands observed at 1400, 2920 and 1840 cm^{-1} (data not shown) confirmed the presence of the wax. However, no sign of the melting point was detected in the corresponding $\Delta\omega$–T_p curve (Fig. 3, right). This indicates that the melting point in this case was dominated by a volume relaxation rather than a change in heat capacity.

Fig. 5 shows that there is a fairly good correlation between the results obtained by DSC and SPM. Fig. 5 also includes values for several reference samples obtained either from the data published by Ihalainen et al. [38] or from additional measurements (data not shown). It should be noted that the reference samples 1–3 are crystalline polymers which do not show T_g but T_m. In general, the surface transition temperature observed by SPM tends to be slightly higher than the bulk transition temperature observed by DSC. This could be due to numerous reasons, including differences in heating rate, bulk versus surface T_g, the interference from the kinetic component, etc. However, the fairly good correlation indicates that the heating-by-the-probe method is able to detect the changes in the effective heat capacity even in complex composite matrices.

3.2. Temperature-induced topographical and material contrast differences

Typical SPM topographic and phase images of the toners before oven-annealing reveal the shape characteristics of the particles (Fig. 6). The polyester toner samples consist of irregular particles, while toner 3 consists of smoother particles with fused structure typical of chemically prepared toners [47]. Respectively, the smallest RMS roughness value (S_q) and the smallest effective surface are (S_{dr}) are found for toner 3 (Table 2).

The toner 1 particles appear homogeneous in the phase image (Fig. 6D). The contrast differences visible at the particle–particle interfacial boundaries are most probably due to topographic contributions to phase shift and can be ignored [48]. The toner 2 particles appear slightly more heterogeneous than toner 1. The clearly most heterogeneous surface was observed for toner 3

Table 2
Roughness parameters determined for toners tablets before and after oven-annealing

Image	S_q (nm)	S_{sk}	S_{dr} (%)
Toner 1 (powder tablet)	593 ± 82	−1.64 ± 0.24	54.1 ± 8.7
Toner 1 (oven-annealed)	17.1 ± 2.1	3.28 ± 1.43	0.1 ± 0.1
Toner 2 (powder tablet)	755 ± 196	−0.84 ± 0.22	76.6 ± 17.0
Toner 2 (oven-annealed)	19.4 ± 3.8	3.79 ± 0.78	2.5 ± 0.4
Toner 3 (powder tablet)	445 ± 10	−1.25 ± 0.23	23.4 ± 4.7
Toner 3 (oven-annealed)	26.9 ± 1.1	0.22 ± 0.23	0.6 ± 0.3

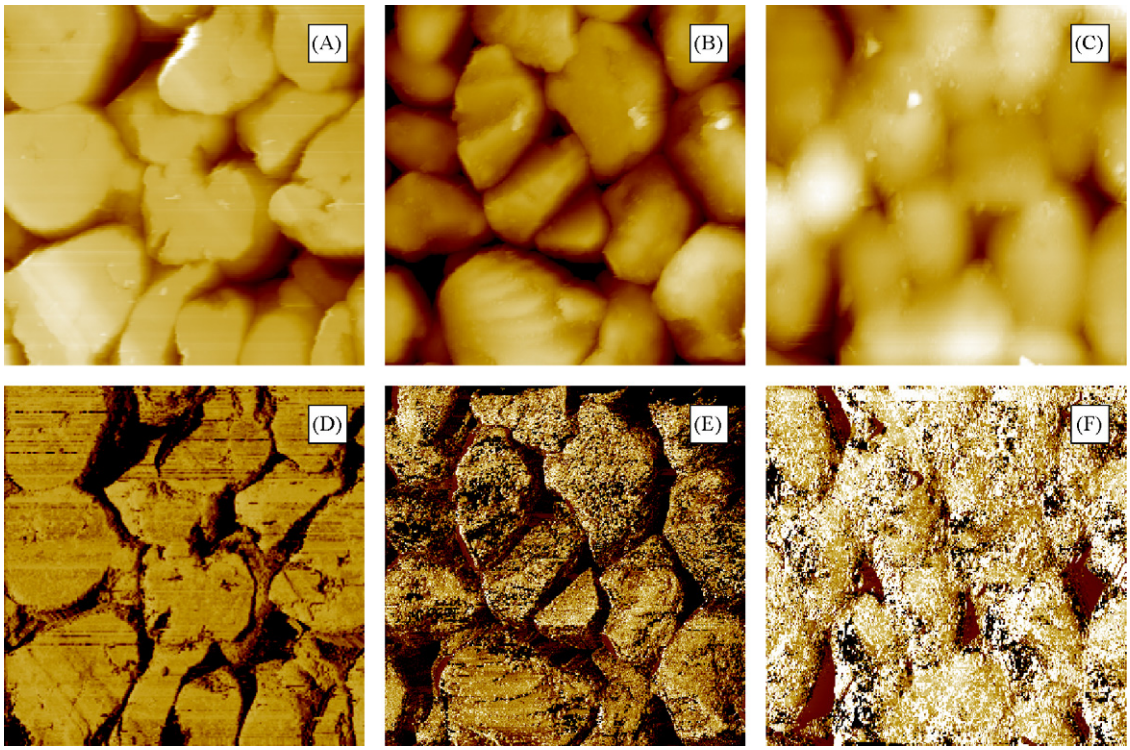

Fig. 6. SPM topography (A–C) and phase (D–F) images of toner samples before being oven-annealed. Topographic height scales: toner 1, 4500 nm; toner 2, 3500 nm; toner 3, 3000 nm. Image size: 25 μm × 25 μm and color contrast in phase images: 50°.

sample (Fig. 6F). The phase contrast differences seen in the image do not completely couple with topographic image and thus the topographic contributions to phase shifts can be concluded to negligible. The toner particles were partly covered by a material which gives higher phase shift (most light-appearing) compared to the toner itself. Phase images were captured in repulsive region, indicating the dominance of repulsive forces (i.e. indentation). Phase shifts are generally known to be insensitive to variations in the elastic properties or adhesion forces and in most cases reflect only the change in amount of energy dissipated by the tip-sample forces due the viscous damping or adhesion energy hysteresis [48–50]. Thus, whether the material covering toner particles is stiffer or softer compared to the background can not be concluded from the phase image. However, in this case the phase image (Fig. 6F) can be considered to be more indicative compared to the topographic image (Fig. 6C) for showing the presence of heterogeneities at the surface. It is believed that the regions with higher phase shift represent inorganic additives (e.g. silica particles) that have penetrated to the toner surface; this interpretation agrees with results presented by Voelkel et al. [51] and Mitsuya et al. [52]. It has also been reported that fumed silica penetrated into the toner matrix are weakly bound silicates that could be removed during a washing sequence with ethanol under ultrasonic treatment [53].

The oven-annealed samples were more than a decade smoother (regarding S_q and S_{dr}) than the non-annealed samples (Table 2). The oven-annealed polyester-based toner films were slightly smoother than the film of the chemical toner (Table 2). It was not possible to identify individual particles, nor any remainders of particle–particle interfaces on the sample surfaces (Fig. 7). The change of porous surfaces to non-porous structures as a result of oven-annealing is not only visualized in Figs. 6 and 7, but also demonstrated as a change of skewness values (S_{sk}) from strongly negative to clearly positive values (Table 2). The film of oven-annealed toner 3 is closest to a Gaussian surface ($S_{sk} \approx 0$).

All the oven-annealed samples appeared quite heterogeneous as concluded from the phase contrast images (Fig. 7D–F). The surface of the film of toner 1 clearly consist of two different phases with very high phase angle difference (Fig. 7D). The phases are quite well mixed not forming distinct areas. In toner 2 film, the surface consisted of particles with darker phase contrast embedded on the matrix giving lighter contrast (Fig. 7E), whereas for toner 3 the film matrix appears very heterogeneous (Fig. 7F). On the contrary to the samples before oven-annealing (Fig. 6), where the phase images were capture in repulsive region (Fig. 6D–F), the phase images for the sample after oven-annealing were forced to obtain in bistable imaging states (attractive-repulsive). However, this did not result any apparent artifacts in the topographs (Fig. 7A–C). Furthermore, topographic coupling did not completely explain the relative large changes in phase contrast. Sudden changes between two imaging states during scanning have been stated to be an indicative of charge interactions between the tip and the sample [54].

Fig. 8 compares the effect of local SPM probe annealing (Fig. 8B) and oven-annealing (Fig. 8C) on the topography of the toner 2 powder tablet (Fig. 8A). With both annealing methods, the surface changed from a rough and porous morphology (Fig. 8A; $S_q = 755$ nm, $S_{sk} = -0.84$) to a smooth, non-porous surface (for Fig. 8B; $S_q = 15.9$ nm, $S_{sk} = 3.9$ and for Fig. 8C;

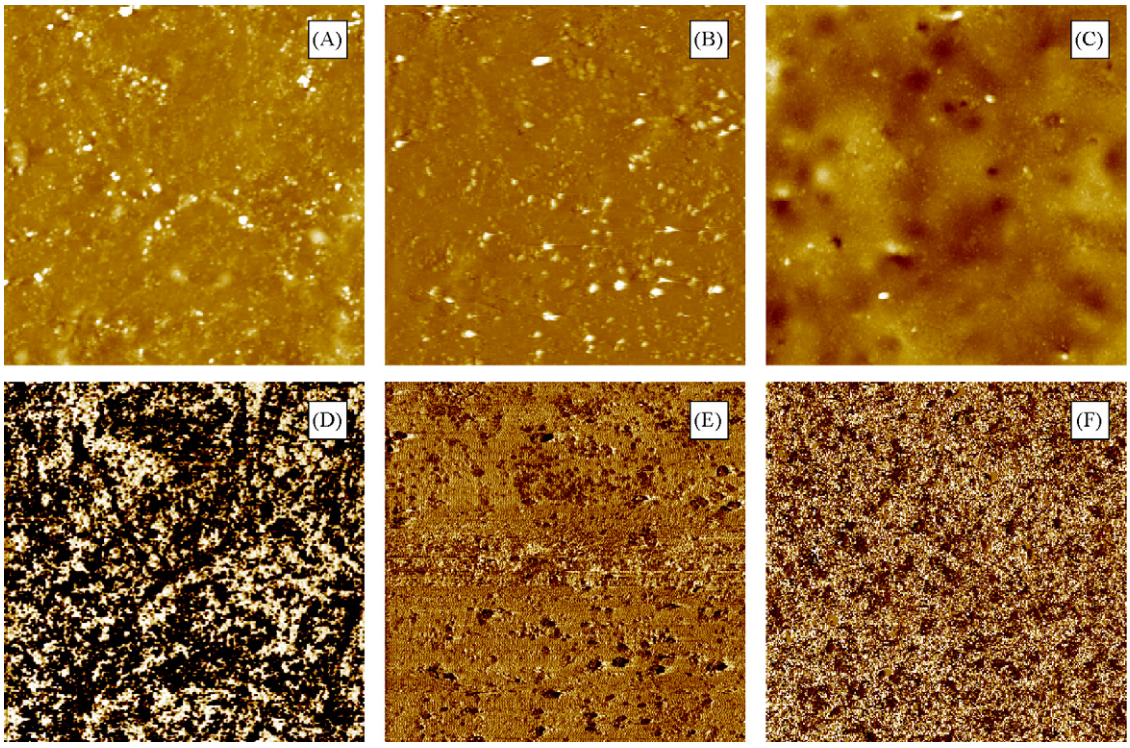

Fig. 7. SPM topography (A–C) and phase (D–F) images of the toner samples after oven-annealing. Topographic height scales: toner 1, 200 nm; toner 2, 300 nm; toner 3, 300 nm. Image size: 25 μm × 25 μm and color contrast in phase images: 50°.

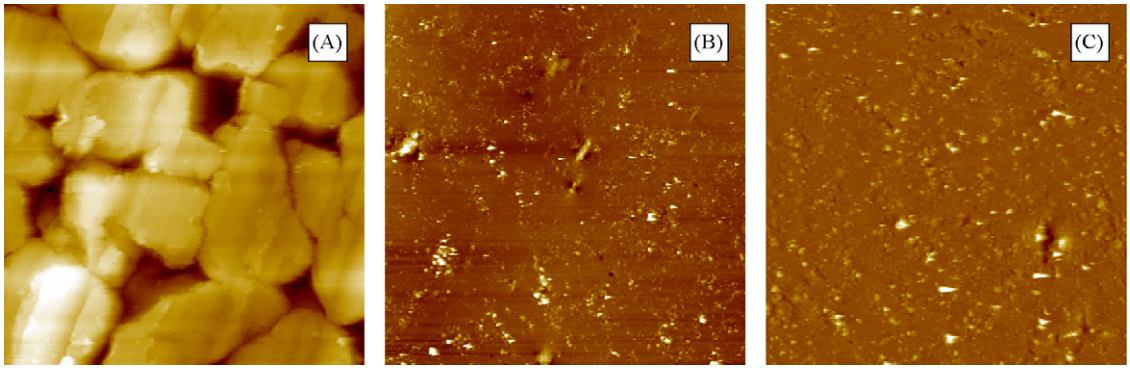

Fig. 8. SPM topography images for toner 2 tablet (powder) (A) before and (B) after SPM probe annealing (100 °C) and (C) after oven-annealing (160 °C). The image size is 25 μm × 25 μm. The height scale in (A) is 4000 nm, and in (B) and (C) 200 nm.

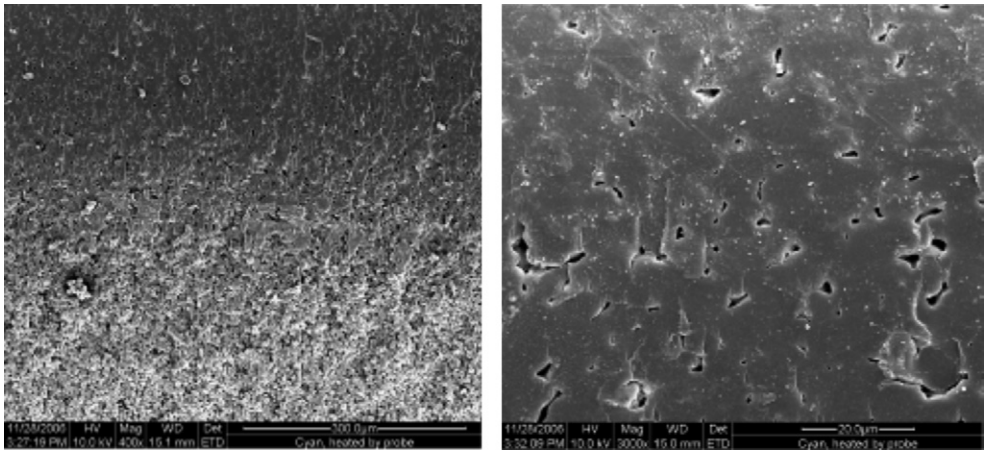

Fig. 9. Cross-section ESEM micrographs of toner samples after SPM probe annealing. Two different magnification were used: The left-hand image (350 μm × 350 μm) and the right-hand image (40 μm × 40 μm).

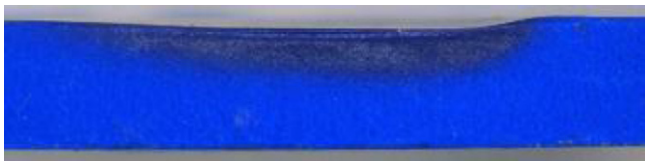

Fig. 10. Microscope image of toner sample after SPM probe analysis. Darker area indicates melted toner particles due to heat radiated from probe tip. Sample thickness is approximately 6 mm.

19.4 nm, $S_{sk} = 3.79$). The result shows that the thermal energy emitted by the SPM probe is enough to cause surface sintering comparable with oven-annealing, even if differences in the thermodynamic behavior were found (Figs. 1–3, Table 1). The small magnification ESEM micrograph (Fig. 9) and the microscope image (Fig. 10), further demonstrates that the heat emitted from the probe has penetrated more than 500 μm into the sample causing detectable changes in the bulk structure (Fig. 9, left). The sealing of the very surface is demonstrated by the large magnification micrograph (Fig. 9, right).

4. Conclusions

We have demonstrated that SPM is a useful method for characterizing thermal properties of polymeric inks such as toners and polymer films. Small changes in heat capacity can be observed and the slow heating rate makes it possible to eliminate the contribution of volumetric changes to the data. This is an indication of a high sensitivity of SPM to detect thermal transitions even though glass transitions are normally associated with only a very small change in heat capacity. Good agreement was found between SPM data and results obtained by Differential scanning calorimetry (DSC). These methods may, however, also be regarded as being complementary; DSC measures bulk properties whereas SPM is a more surface-sensitive method. Besides thermodynamics, SPM provided information about the structural changes involved in a thermal transition. When the thermal history of the samples was considered, interesting results were obtained providing valuable information about the progress of the particle sintering. For the non-annealed toner samples, the heat capacity was found to be characteristic for the toner and especially for the type of binder in the toner. For the oven-annealed samples the differences in heat capacity were much more marginal. Annealing did, however, have an influence on the transition temperature, but also these changes were characteristic of the studied sample. The topographical data complemented the study by enabling to conclude about the progress of the heating-induced sintering process.

Acknowledgements

TEKES is acknowledged for financial support of the project. Dr. Anthony Bristow is thanked for the linguistic revision of the manuscript.

References

[1] H.L. Lee, in: L.H. Lee (Ed.), Adhesion Science and Technology, Plenum Press, 1975, pp. 831–852.
[2] J. van Daele, L. Veruyten, E. Soulliaeryt, IS&Tís NIP12, Springfield, VA, 1996, p. 382.
[3] T. Harthus, Graphic Arts in Finland, vol. 30, 2001, p. 3.
[4] T. Petterson, Wetting and levelling of toner during fusing of electrophotographic prints, Licentiate Thesis, Stockholm, 2004.
[5] J. Lahti, Dry toner based electrophotographic printing on extrusion coated paperboard, Doctoral Thesis, Tampere University of Technology, Tampere, 2005.
[6] L.D. Leroy, Adhesion at toner–paper interface in electrophotographic printing, Doctoral Thesis, Grenoble, 2002.
[7] D.J. Sanders, D.F. Rutland, W.K. Istone, J. Imag. Sci. Technol. 40 (1996) 175–179.
[8] S. Juntunen, J. Virtanen, Proceedings of the TAGA, Rochester, USA, 1991.
[9] R. Appel, J. Knott, M. Scheusener, B. Petschik, Proceedings of the Imaging Science and Technology Conference on Non-impact Printing, vol. 9, 1995, pp. 483–485.
[10] Y. Kuo, Polym. Eng. Sci. 24 (2004) 662–672.
[11] S.S. Hwang, J. Imag. Sci. Technol. 44 (2000) 26–30.
[12] I.L. Britto, Proceedings of the IS&Tís 7th International Congress on Advances in Non-impact Printing Technologies, vol. 1, 1991.
[13] T. Satoh, T. Kawanishi, R. Shimizu, N. Kinjo, J. Imag. Sci. Technol. 35 (1991) 373–376.
[14] T. Mitsuya, M.L. Hunt, Powder Technol. 92 (1997) 119–125.
[15] S. Simula, Electrical and thermal properties of paper, Doctoral Thesis, Helsinki University, Helsinki, 1999.
[16] M. Samei, K. Takenouchi, T. Shimokawa, K. Kawakita, Proceedings of the IS&Tís NIP, vol. 15, 1999.
[17] T.J. Lever, D.M. Price, Am. Lab. (August, 1998).
[18] H. Fischer, Macromolecules 38 (2005) 844–850.
[19] C. Wang, Thermochim. Acta 423 (2004) 89–97.
[20] V.V. Tsukruk, V.V. Gorbunov, N. Fuchigami, Thermochim. Acta 395 (2003) 151–158.
[21] M. Lemieux, S. Minko, D. Usov, M. Stamm, V.V. Tsukruk, Langmuir 19 (2003) 6126–6134.
[22] I. Luzinov, D. Julthongpiput, V.V. Tsukruk, Polymer 42 (2001) 2267–2273.
[23] H.M. Pollock, A. Hammiche, J. Phys. D: Appl. Phys. 34 (2001) R23–R53.
[24] A. Hammiche, M. Reading, H.P. Pollock, M. Song, D.J. Hourston, Rev. Sci. Instrum. 67 (1996) 4268–4274.
[25] B.A. Nelson, W.P. King, Rev. Sci. Instrum. 78 (2007) 1–8, 023702.
[26] B. Gotsmann, U. Dürig, Langmuir 20 (2004) 1495–1500.
[27] F. Dinelli, C. Buenviaje, R.M. Overney, Thin Solid Films 396 (2001) 138–144.
[28] J. Hammerschmidt, W. Gladfelter, G. Haugstadt, Macromolecules 32 (1999) 3360–3367.
[29] K. Tanaka, A. Taura, S. Ge, A. Takahara, T. Kajiyama, Macromolecules 29 (1996) 3040–3042.
[30] S. Sills, R.M. Overney, W. Chau, V.Y. Lee, R.D. Miller, J. Frommer, J. Chem. Phys. 120 (2004) 5334–5338.
[31] S. Ge, Y. PU, W. Zhang, M. Rafailovich, J. Sokolov, C. Buenviaje, R. Buckmaster, R. Overney, Phys. Rev. Lett. 85 (2000) 2340–2343.
[32] F. Oulevey, N. Burnham, G. Gremaud, A. Kulik, H.M. Pollock, A. Hammiche, M. Reading, M. Song, D. Hourston, Polymer 41 (2000) 3087–3092.
[33] V. Bliznyuk, H. Assender, G. Briggs, Macromolecules 35 (2002) 6613–6622.
[34] M. Meincken, R.D. Sanderson, S. Afr. J. Sci. 100 (2004) 256–260.
[35] M. Meincken, L.J. Balk, R.D. Sanderson, Surf. Interface Anal. 35 (2003) 1034–1040.
[36] M. Meincken, S. Graef, K. Mueller-Nedebock, R.D. Sanderson, Appl. Phys. A 74 (2002) 275–371.
[37] M. Meincken, L.J. Balk, R.D. Sanderson, Macromol. Mater. Eng. 286 (2001) 412–420.

[38] P. Ihalainen, K. Backfolk, P. Sirviö, J. Peltonen, J. Appl. Phys. 101 (2007) 1–10, 043505.
[39] K. Backfolk, R. Holmes, P. Ihalainen, P. Sirviö, N. Triantafillopoulus, J. Peltonen, Polymer Testing 26 (2007) 1031–1040.
[40] P. Ihalainen, K. Backfolk, P. Sirviö, J. Peltonen, J. Appl. Polym. Sci., in press.
[41] Veeco Metrology Group, Support Note 297, Rev. D, 2001.
[42] D.A. Ivanov, Z. Amalou, S.N. Magonov, Macromolecules 34 (2001) 8944–8952.
[43] D.A. Ivanov, R. Daniels, S.N. Magonov, Exploring the High Temperature AFM and Its Use for Studies of Polymers, Application Notes 45, Rev. A1, Veeco Instruments Inc., 2004.
[44] G. Forgo, M. Ragnetti, A. Stubbe, J. Imag. Sci. Technol. 37 (1993) 176–186.
[45] M. Song, D.J. Hourston, G.G. Silva, I.C. Machado, J. Polym. Sci. B: Polym. Phys. 39 (2001) 1659–1664.
[46] J. Brandrup, E.H. Immergut, E.A. Grulke, Polymer Handbook, 4th edition, John Wiley & Sons, 1999.
[47] G.J. Galliford, Proceedings of the 5th Annual Toner Ink Jet & Imaging Chemicals Conference, Florida, USA, 2002.
[48] R. García, R. Pérez, Surf. Sci. Rep. 47 (2002) 197–301.
[49] R. García, J. Tamayo, A.S. Paulo, Surf. Interface Anal. 27 (1999) 312–316.
[50] J. Tamayo, R. Garcia, Appl. Phys. Lett. 71 (1997) 2394–2396.
[51] U. Voelkel, H. Barthel, M. Heinemann, Proceedings of the 5th Annual Toner Ink Jet & Imaging Chemicals Conference, Florida, USA, 2002.
[52] T. Mitsuya, T. Kumasaka, S. Fujiwara, S. Nishino, Opt. Eng. 30 (1991) 111–116.
[53] M. Heinemann, Proceedings of the 5th Annual Toner S Ink, Jet Ink & Imaging Chemicals Conference, Orlando, USA, February 13–15, 2002.
[54] P.J. James, M. Antognozzi, J. Tamayo, T.J. McMaster, J.M. Newton, M.J. Miles, Langmuir 17 (2001) 349–360.